

Compression and pressure-induced amorphization of $\text{Co}(\text{OH})_2$ characterized by infrared vibrational spectroscopy

Jeffrey H. Nguyen

Physics Department, University of California at Berkeley, Berkeley, California 94720

Michael B. Kruger* and Raymond Jeanloz

Department of Geology and Geophysics, University of California at Berkeley, Berkeley, California 94720

(Received 5 August 1993)

The infrared-active (A_{2u}) O-H vibration of $\text{Co}(\text{OH})_2$ decreases in frequency under hydrostatic compression to 51 GPa at 290 K. Similarly, the bond anharmonicity, determined from the $\nu_1 \rightarrow \nu_2$ absorption-band difference, increases by more than a factor of 2 between 0 and 20 GPa. Both changes are attributed to an increase in the O-H bond length due to enhanced hydrogen bonding under pressure. The full width at half maximum (FWHM) of the fundamental absorption band increases abruptly by $\sim 100 \text{ cm}^{-1}$ at $11.2 (\pm 0.3) \text{ GPa}$, and continues to increase at a rate of $\sim 3.3 \text{ cm}^{-1}/\text{GPa}$ up to 36 GPa. Above $36 (\pm 2) \text{ GPa}$ and below the onset of amorphization, the FWHM changes at a slower rate, $0.8 (\pm 0.1) \text{ cm}^{-1}/\text{GPa}$. The abrupt change in FWHM is reversible on decompression, and is interpreted in terms of a pressure-induced crystal-to-glass transition exhibiting a small hysteresis compared to similar compounds. The rapid variation in FWHM above the transition pressure suggests that the amorphous structure is continuously modified between 11.3 and 36 GPa.

INTRODUCTION

Infrared vibrational spectra document that the hydrogen bonding in $\text{Mg}(\text{OH})_2$ and $\text{Ca}(\text{OH})_2$ is enhanced under pressure.¹ Moreover, $\text{Ca}(\text{OH})_2$ undergoes pressure-induced amorphization at about 12 GPa, whereas the isostructural $\text{Mg}(\text{OH})_2$ remains crystalline up to at least 34 GPa.¹⁻³ It is unclear whether or not the differences in amorphization conditions can be explained simply through geometrical considerations (e.g., differences in ionic radii and crystalline packing fractions).

$\text{Co}(\text{OH})_2$ is examined here to further characterize the hydroxide family under pressure, and specifically to document the effects, if any, of changing the cation from an alkaline earth to a transition metal. As the ionic radius of Co (0.65 \AA and 0.75 \AA for low and high spin, respectively)⁴ is close to that of Mg (0.72 \AA),⁴ and distinctly less than that of Ca (1.00 \AA),⁴ simple considerations of ionic radii would suggest that if $\text{Co}(\text{OH})_2$ amorphizes, it should do so only at pressure greater than 34 GPa.¹

$\text{Co}(\text{OH})_2$ is isostructural with $\text{Mg}(\text{OH})_2$ brucite [Fig. 1(a)], crystallizing in the CdI_2 structure with D_{3d}^3 ($P3m$) symmetry.⁵ Viewed along the c direction, the Co ion is at the center of a puckered hexagon, with the hydroxides (oriented along the c direction) being at the corners. Viewed in a direction perpendicular to the c axis, the hydroxides form planes alternately above and below that of the Co ions. Adjacent hydroxide planes are held together by weak interactions between the neighboring OH "ions." Factor-group analysis of $\text{Co}(\text{OH})_2$ determines that there are two allowed normal modes of vibration, the Raman-active A_{1g} mode and the infrared-active A_{2u} mode⁶ [Fig. 1(b)]. The former is an in-phase stretching of the hydroxides while the latter is an out-of-phase stretch-

ing. At zero pressure, the frequency of the infrared-active mode is observed at $3631 \pm 3 \text{ cm}^{-1}$. A previous study placed this frequency at 3629 cm^{-1} .⁷

It has been proposed that an unperturbed OH^- mole-

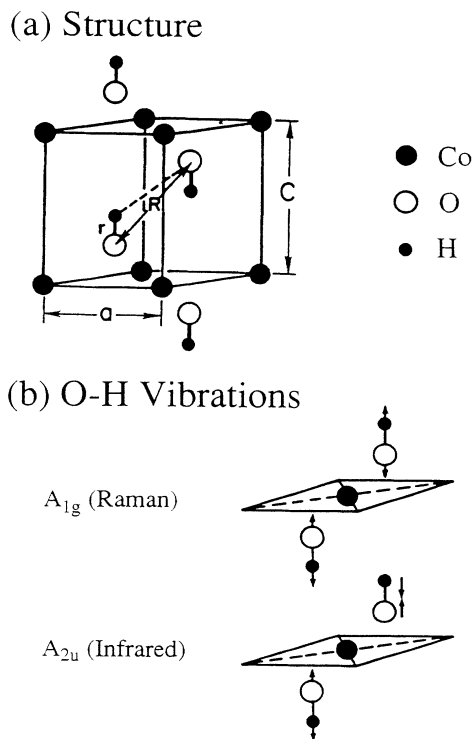


FIG. 1. (a) Structure of $\text{Co}(\text{OH})_2$. The larger closed circles represent Co atoms, the smaller closed circles H atoms, and the open circles are oxygen atoms. The hydrogen bond is shown by the dashed line. (b) Internal vibrational modes of hydroxyl bonds.

cule vibrates at $3570 \pm 10 \text{ cm}^{-1}$.⁸ The increases in O-H vibrational frequency of ionic hydroxides, such as $\text{Ca}(\text{OH})_2$ and $\text{Mg}(\text{OH})_2$ (3633 and 3670 cm^{-1} , respectively), are thought to be due to repulsive effects of the lattice. If hydrogen bonding is present, the vibrational frequencies are expected to decrease instead.⁸ Thus, one would conclude that hydrogen bonding is very weak, if present at all, in $\text{Co}(\text{OH})_2$ because the observed O-H frequency is some 60 cm^{-1} higher in the crystal than for the unperturbed molecule.

EXPERIMENT

Reagent-grade $\text{Co}(\text{OH})_2$ (97% purity, Johnson Matthey Catalog Company, Ward Hill, MA) was loaded into a gasketed Mao-Bell-type diamond-anvil cell.⁹ The diamond culets were $350 \mu\text{m}$ in diameter and, initially, the gasket hole was $200 \mu\text{m}$ in diameter and about $50 \mu\text{m}$ in thickness. A few grains of ruby were added for measuring pressure using the ruby-fluorescence technique.^{10,11} For each run, the pressure was determined at 3–5 different locations in the sample chamber to insure adequate characterization of the nonhydrostatic stress state. All experiments were performed at room temperature (290 K).

Two different materials, Ar and CsI, were used as pressure-transmitting media. In the experiment with Ar as a medium, the pressure was initially raised to 11 GPa and then increased in steps of approximately 5 GPa (after each measurement) up to a peak pressure of 51 GPa. The sample pressure was then decreased with the same pressure intervals, down to about 0.8 GPa. When CsI was used as a pressure-transmitting medium, $\text{Co}(\text{OH})_2$ was mixed with and diluted by CsI [1.0% $\text{Co}(\text{OH})_2$ by weight]. Pressure was then increased until nonhydrostaticity became evident, as documented by measurable pressure variations across the sample. In the region where CsI is relatively hydrostatic ($< 12 \text{ GPa}$), the results using both pressure media agreed to within our quoted uncertainties.

A Bomem DA3.02 and a Bruker IFS 66V Fourier-transform infrared (FTIR) spectrometer with a global source and liquid- N_2 -cooled InSb detector were used to collect absorption spectra over a frequency range from 2000 to 5000 cm^{-1} . The apodized resolution for all spectra in this study is 4 cm^{-1} . An additional infrared spectrum was collected from a sample at zero pressure using a Cary 2390 grating spectrophotometer.

RESULTS AND DISCUSSION

A. Reversible amorphization

Representative infrared absorption spectra are presented in Fig. 2. The more intense peak is due to absorption from the fundamental infrared-active vibration having A_{2u} symmetry.⁶ The source of the weaker peak will be discussed in the following section. Of particular interest is the variation in full width at half maximum (FWHM) as a function of pressure (Fig. 3).

On compression, the FWHM broadens by nearly an or-

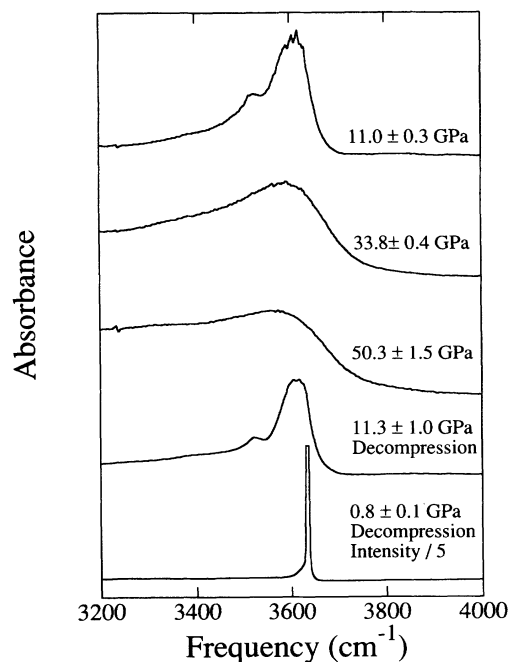


FIG. 2. Typical infrared absorption spectra of $\text{Co}(\text{OH})_2$ taken under pressure. The intensity of the 0.8-GPa spectrum is divided by 5. The hot band is present in the 0.8-GPa spectrum, but its intensity is much smaller than that of the main vibrational peak and is not visible in this plot.

der of magnitude, from about 20 to over 120 cm^{-1} at $11.2 \pm 0.3 \text{ GPa}$. A dramatic increase in the FWHM of the infrared-active O-H stretching vibration has been previously observed for $\text{Ca}(\text{OH})_2$.¹ This behavior was attributed to amorphization of the crystal, as confirmed by x-ray diffraction.^{1,12} Based upon these previous observa-

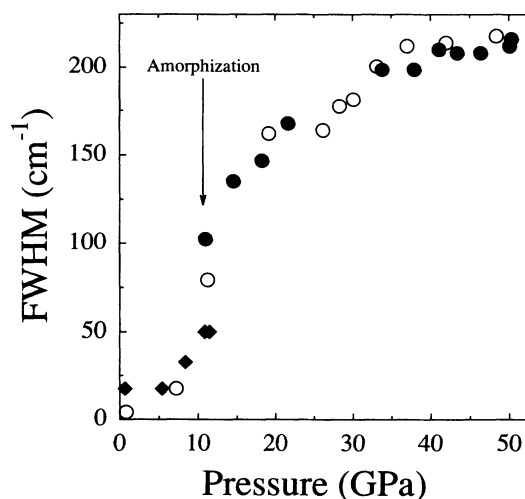


FIG. 3. Full width at half maximum (FWHM) of the fundamental mode, with closed (open) symbols representing data taken on compression (decompression). Data using an Ar medium are shown as circles; CsI medium as diamonds. Amorphization is observed at $11.2 \pm 0.3 \text{ GPa}$ where there is a jump in the FWHM of the excitation. On decompression, the sample returns to the crystalline state with small hysteresis. Uncertainty for FWHM is less than 10% of its value; pressure uncertainty is less than 1.5 GPa for most measurements.

tions we conclude that $\text{Co}(\text{OH})_2$ undergoes pressure-induced amorphization. The resulting disorder in the glass, including a broad distribution of O-H distances, causes a manifold of closely spaced O-H resonant frequencies that accounts for the increased FWHM.

Amorphization of $\text{Co}(\text{OH})_2$ at such low pressures is unexpected based upon ionic radii arguments. The Mg^{2+} ion in $\text{Co}(\text{OH})_2$ has an atomic radius of 0.72 Å, whereas the atomic radius of the Co^{2+} ion is 0.65 Å in $\text{Co}(\text{OH})_2$. Thus the standard assumption that transformation pressures are proportional to cation radii appears not to apply in this situation.¹

The FWHM continues to increase with pressure at a rate of $\sim 3.3 \text{ cm}^{-1}/\text{GPa}$ between 11.2 ± 0.3 and 36 ± 2 GPa. Outside this pressure range, both below the amorphization pressure and above 36 GPa, the FWHM increases at the much lower rate of $\sim 0.8 \text{ cm}^{-1}/\text{GPa}$. This indicates that there are rapid changes in the local structure of the sample over a pressure interval ranging to ~ 25 GPa above the amorphization transition. Unlike $\text{Ca}(\text{OH})_2$, we see no evidence of coexisting crystalline and amorphous materials (i.e., superimposed spectra) over this pressure interval. Therefore, we infer that the amorphous structure formed on compression to 11.2 GPa is further modified as pressure is increased to 36 GPa. Multiple transformations to high-pressure noncrystalline phases were similarly observed in $\text{Ca}(\text{OH})_2$.¹³ Since the pressure range (~ 25 GPa) is approximately an order of magnitude greater than the maximum pressure gradient across the face of the diamond (~ 1.7 GPa), we can conclude that disordering is primarily due to hydrostatic pressure, with shearing of the sample playing at most a minor role.

As the pressure is lowered, the FWHM decreases, essentially retracing the path taken on compression. Since the FWHM returns to a low value ($\sim 20 \text{ cm}^{-1}$) characteristic of the crystalline phase, we conclude that the high-pressure amorphous phase reverts to the crystalline state upon decompression. The small hysteresis (< 2 GPa) observed in $\text{Co}(\text{OH})_2$ is apparently unique: for all previously reported crystalline-amorphous transitions, a large amount of hysteresis is present.^{14–21}

B. Hydrogen bonding

As shown in Fig. 4, the vibrational frequency decreases by approximately 40 cm^{-1} when the sample undergoes the initial transformation to a high-pressure amorphous phase at 11.2 ± 0.3 GPa. Such a drop in vibrational frequency at the amorphization pressure has been observed previously, and is attributed to an increase in the strength of the $\text{O} \cdots \text{H}$ hydrogen bond.^{1,22} Shifts in $\text{O} \cdots \text{H}$ frequency under application of pressure have also been observed in organic solids.²³

A simple model for hydrogen-bond enhancement can be obtained with two Morse potentials.^{1,23} In such a model, the interactions of the hydrogen atom with the two adjacent oxygen hosts can be approximated by $V_1 = D[1 - \exp(-nDr^2/2r)]$ and $V_2 = -D^* \{1 - \exp[-n^*(R - r - r_0)^2/2(R - r)]\}$ for the strong and weak O-H bonds, respectively.²⁴ D and D^*

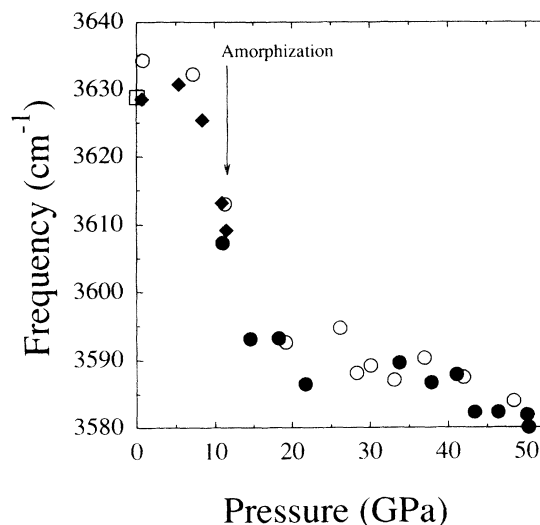


FIG. 4. Hydrogen-bond enhancement. Closed (open) symbols represent data taken on compression (decompression). Data with CsI as the pressure medium are shown as diamonds. The square represents datum from a previous study at zero pressure (Ref. 7). At amorphization point, 11.2 ± 0.3 GPa, a steep drop in the vibrational frequency is observed. Uncertainty in frequency measurement is less than 3 cm^{-1} .

are bond strengths, r_0 is the equilibrium O-H distance for a free hydroxyl group, and R and r are the bond lengths of the two O-H bonds (Fig. 1). Van der Waals and repulsive forces are negligible in this calculation, and are thus ignored.^{1,24} Though the $\text{O-H} \cdots \text{O}$ bond is not linear, an approximately linear bond is used for the sake of simplicity. Moreover, the $\text{O-H} \cdots \text{O}$ hydrogen bond in $\text{Ca}(\text{OH})_2$, a close relative of $\text{Co}(\text{OH})_2$, is thought to be nearly linear.²⁵

Since the ionic radius of Co is close to that of Mg,⁴ one can use the two Morse-potential parameters of Ref. 24 and the shock-wave data for $\text{Mg}(\text{OH})_2$ from Simakov *et al.*²⁶ to calculate $\partial P/\partial \nu$.¹ From such a calculation, we would expect the O-H vibrational frequency to decrease at a rate of $\sim 5 \text{ cm}^{-1}/\text{GPa}$. Decompression data, however, show that the vibrational frequency decreases at a rate of $0.4 \pm 0.1 \text{ cm}^{-1}/\text{GPa}$ after amorphization has taken place. Though the result does not agree numerically, we obtain a theoretical value that agrees in sign and is within an order of magnitude of the observed pressure shift of the vibrational frequency.

Using this two-Morse-potential model, we expect that the vibrational frequency decreases with R as r increases. Lippincott and Schroeder²⁴ have shown that as the O-O distance (R) decreases r increases and the vibrational frequency decreases. Our result exhibits this decrease in vibrational frequency. Strong hydrogen bonding in crystals has been shown to exist by Rundle and Parasol,²⁷ Lord and Merrifield,²⁸ and more recently by Kruger, Williams, and Jeanloz.¹

C. Anharmonicity

In addition to the main absorption peak, a secondary peak of low intensity is also observed, either when the

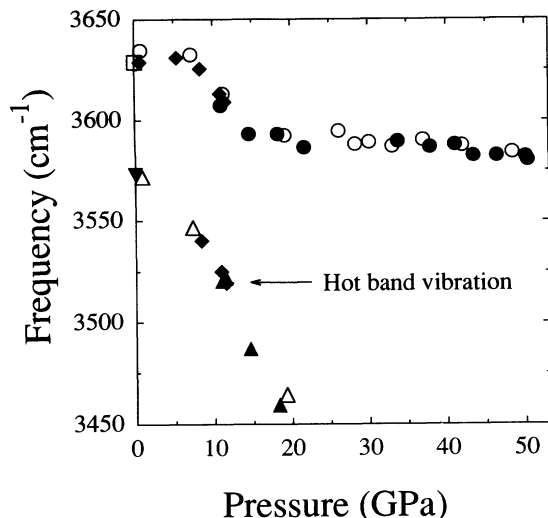


FIG. 5. Vibrational frequencies of the fundamental mode (upper line) and hot band (lower line) as a function of pressure. Closed symbols represent data taken on compression; open symbols stand for those on decompression. Diamonds are used for data taken with CsI as the pressure medium. The result of a previous study (Ref. 7) at zero pressure is shown as a square. The data point represented by the inverted triangle indicates the hot band observed at zero pressure. Both frequencies decrease with increasing pressure, indicating increased hydrogen bonding with pressure. The hot band is observed distinctly only at low pressures due to low signal intensity at higher pressures.

sample is not compressed or when the pressure is less than 20 GPa (Figs. 2 and 5). To help ascertain the origin of the second absorption band, infrared absorption spectra of the same sample were collected at 0 GPa using a grating spectrometer and a FTIR spectrometer. The additional peak was not observed in the spectrum collected with the grating spectrometer. We thus conclude that this peak, observable only with the polychromatic il-

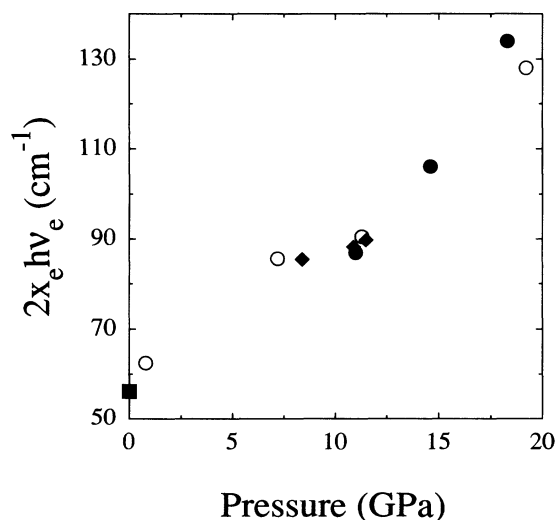


FIG. 6. Anharmonicity of the O-H bond as a function of pressure. Closed symbols represent data taken on compression; open symbols stand for those on decompression. Diamonds and square are for data with CsI as the pressure medium.

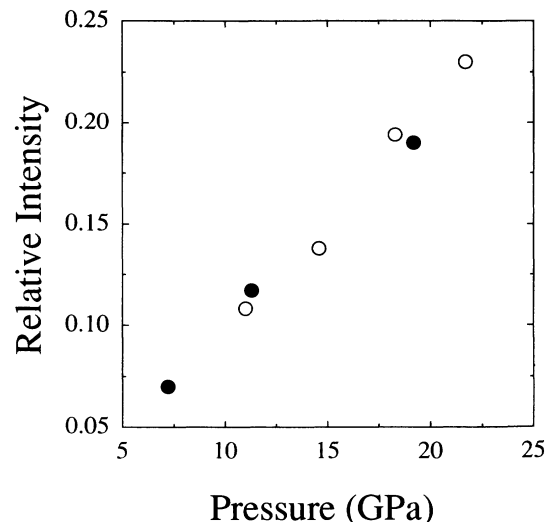


FIG. 7. Ratio of the hot-band amplitude to that of the fundamental peak. The ratio approaches 0 at zero pressure. At pressures above 20 GPa, the amplitudes of the hot band and the fundamental mode are too weak to be measured with any degree of certainty.

lumination of the FTIR, is a hot band; that is, an absorption resulting from the $n = 1$ to $n = 2$ transition. Such hot bands have been previously seen in $\text{Mg}(\text{OH})_2$.¹

Knowing both the fundamental and hot-band frequencies, one can determine the anharmonicity as a function of pressure. Assuming only a first-order anharmonic factor, the energy of the n th level, E_n , can be represented as,

$$E_n = h\nu_e(n + 1/2) + x_e h\nu_e(n + 1/2)^2,$$

where ν_e is the frequency for oscillation around the equilibrium position, h is Planck's constant, and x_e is the anharmonic factor.²⁹ The difference in the measured frequencies of the fundamental mode and the hot band is proportional to the anharmonic factor $2x_e h\nu_e$, which is seen to increase rapidly with compression (Fig. 6). Furthermore, as pressure is raised, the amplitude of the hot band increases relative to that of the fundamental band (Fig. 7). This effect has been observed previously in $\text{Mg}(\text{OH})_2$, and was also attributed to anharmonic effects.¹

CONCLUSION

An infrared absorption study of $\text{Co}(\text{OH})_2$ confirms many of the high-pressure results observed among other hydroxides. In particular, reversible amorphization occurs at 11.2 ± 0.3 GPa, with further modification of the disordered state continuing up to 36 ± 2 GPa. Amorphization is accompanied by an enhancement of the hydrogen-bond strength, and an increase in the anharmonicity of the O-H bond. Thus, substituting a transition metal for an alkaline-earth cation does not significantly change the high-pressure behavior of the hydroxide compound.

ACKNOWLEDGMENTS

We wish to thank Dr. J. Wolk for his help in collecting the infrared absorption spectra with the Cary grating spectrometer. This work was supported by NASA and NSF.

*Present address: Department of Physics, University of Missouri–Kansas City, Kansas City, MO 64110.

- ¹M. B. Kruger, Q. Williams, and R. Jeanloz, *J. Chem. Phys.* **91**, 5910 (1989).
- ²T. S. Duffy and T. J. Ahrens, *J. Geophys. Res.* **96**, 14 319 (1991).
- ³Y. Fei and H. K. Mao, *J. Geophys. Res.* **98**, 11 875 (1993).
- ⁴L. Liu and W. A. Bassett, *Elements, Oxides, Silicates: High Pressure Phases with Implications for the Earth's Interior* (Oxford University Press, New York, 1986), pp. 12–13.
- ⁵H. D. Megaw, *Crystal Structures: A Working Approach* (Saunders, Philadelphia, 1972).
- ⁶S. S. Mitra, *Solid State Physics*, edited by F. Seitz and D. Turnbull (Academic, New York, 1962), Vol. 13, p. 1.
- ⁷A. A. Tsyganenko, *Zh. Strukt. Khim.* **16**, 572 (1975).
- ⁸H. D. Lutz, W. Eckers, and H. Haeuseler, *J. Mol. Struct.* **80**, 221 (1982).
- ⁹H. K. Mao, P. M. Bell, K. J. Dunn, R. M. Chrenko, and R. C. DeVries, *Rev. Sci. Instrum.* **50**, 1002 (1979).
- ¹⁰G. J. Piermarini, S. Block, J. D. Barnett, and R. A. Forman, *J. Appl. Phys.* **46**, 2774 (1975).
- ¹¹H. K. Mao, P. B. Bell, J. W. Shaner, and D. J. Steinberg, *J. Appl. Phys.* **49**, 3276 (1978).
- ¹²C. Meade and R. Jeanloz, *Geophys. Res. Lett.* **17**, 1157 (1990).
- ¹³C. Meade, R. Jeanloz, and R. J. Hemley, in *High Pressure Research: Application to Earth and Planetary Sciences*, edited by Y. Syono and M. H. Manghnani (Terra Scientific, Tokyo, 1992), pp. 485–496.
- ¹⁴M. B. Kruger and R. Jeanloz, *Science* **249**, 647 (1990).
- ¹⁵U. Fujii, M. Kowaka, and A. Onodera, *J. Phys. C* **18**, 789 (1985).
- ¹⁶H. Sankaran, S. M. Sharma, S. K. Sikka, and R. Chidambaram, *Paramana* **35**, 177 (1990).
- ¹⁷H. Sankaran, S. K. Sikka, S. M. Sharma, and R. Chidambaram, *Phys. Rev. B* **38**, 170 (1988).
- ¹⁸C. Meade and R. Jeanloz, *Science* **252**, 68 (1991).
- ¹⁹S. Sugai, *J. Phys. C* **18**, 799 (1985).
- ²⁰A. Jayaraman, D. L. Wood, and R. G. Maines, *Phys. Rev. B* **35**, 8316 (1987).
- ²¹C. Meade and R. Jeanloz, *Geophys. Res. Lett.* **17**, 1157 (1990).
- ²²J. R. Feraro, *Vibrational Spectroscopy at High External Pressures: The Diamond Anvil Cell* (Wiley, New York, 1986).
- ²³S. H. Moon and H. G. Drickamer, *J. Chem. Phys.* **61**, 48 (1974).
- ²⁴E. R. Lippincott and R. Schroeder, *J. Chem. Phys.* **23**, 1099 (1955).
- ²⁵K. Nakamoto, M. Margoshes, and R. E. Rundle, *J. Am. Chem. Soc.* **77**, 6480 (1955).
- ²⁶G. V. Simakov, M. N. Pavlovskiy, N. G. Kalashiniko, and R. F. Trunin, *Phys. Sol. Earth* **448**, 10 (1974).
- ²⁷R. E. Rundle and M. Parasol, *J. Chem. Phys.* **20**, 1487 (1992).
- ²⁸R. C. Lord and R. E. Merrifield, *J. Chem. Phys.* **21**, 166 (1953).
- ²⁹C. Cohen-Tannoudji, B. Diu, and F. Laloë, *Quantum Mechanics* (Wiley, New York, 1977), Vols. 1 and 2.